European Journal of Pharmacology 945 (2023) 175612

Contents lists available at ScienceDirect

European Journal of Pharmacology

journal homepage: www.elsevier.com/locate/ejphar

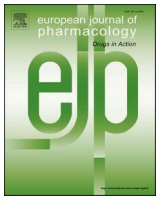

The molecular mechanisms of apoptosis accompanied with the epigenetic regulation of the NY-ESO-1 antigen in non-small lung cancer cells treated with decitabine (5-aza-CdR)

Varghese P. Inchakalody [a,b], Shereena P. Hydrose [a,b], Roopesh Krishnankutty [c], Maysaloun Merhi [a,b], Lubna Therachiyil [c,k], Varun Sasidharan Nair [f], Asma A. Elashi [g], Abdul Q. Khan [c], Sara Taleb [e], Afsheen Raza [a,b], Zeenath Safira K.M. Yoosuf [b,g], Queenie Fernandes [b,h], Lobna Al-Zaidan [a,b], Sarra Mestiri [a,b], Nassiba Taib [a,b], Takwa Bedhiafi [a,b], Dina Moustafa [a,b], Laila Assami [a,b], Karama Makni Maalej [a,b], Eyad Elkord [i,j], Shahab Uddin [c,d], Ussama Al Homsi [a,b], Said Dermime [a,b,*]

[a] National Center for Cancer Care and Research, Hamad Medical Corporation, Doha, Qatar
[b] Translational Cancer Research Facility, Interim Translational Research Institute, Hamad Medical Corporation, Doha, Qatar
[c] Translational Research Institute, Academic Health System, Hamad Medical Corporation, Doha, Qatar
[d] Translational Research Institute and Dermatology Institute, Academic Health System, Doha, Qatar
[e] Genomics and Precision Medicine, Hamad Bin Khalifa University, Doha, Qatar
[f] Department of Experimental Immunology, Helmholtz Centre for Infection Research, Germany
[g] College of Health and Life Sciences, Hamad Bin Khalifa University, Doha, Qatar
[h] College of Medicine, Qatar University, Doha, Qatar
[i] Natural and Medical Sciences Research Center, University of Nizwa, Oman
[j] Biomedical Research Center, School of Science, Engineering and Environment, University of Salford, Manchester, UK
[k] College of Pharmacy, Qatar University, Doha, Qatar

ARTICLE INFO

Keywords:
Non small lung cancer
5 Aza-CdR
Epigenetic regulation
NY-ESO-1
Apoptosis
Intrinsic and extrinsic apoptotic pathway

ABSTRACT

Dysregulated epigenetic modifications are common in lung cancer but have been reversed using demethylating agent like 5-Aza-CdR. 5-Aza-CdR induces/upregulates the NY-ESO-1 antigen in lung cancer. Therefore, we investigated the molecular mechanisms accompanied with the epigenetic regulation of *NY-ESO-1* in 5-Aza-CdR-treated NCI–H1975 cell line. We showed significant induction of the NY-ESO-1 protein (**$p < 0.0097$) using Cellular ELISA. Bisulfite-sequencing demonstrated 45.6% demethylation efficiency at the *NY-ESO-1* gene promoter region and RT-qPCR analysis confirmed the significant induction of *NY-ESO-1* at mRNA level (128-fold increase, *$p < 0.050$). We then investigated the mechanism by which 5-Aza-CdR inhibits cell proliferation in the NCI–H1975 cell line. Upregulation of the death receptors TRAIL (2.04-fold *$p < 0.011$) and FAS (2.1-fold *$p < 0.011$) indicate activation of the extrinsic apoptotic pathway. The upregulation of Voltage-dependent anion-selective channel protein 1 (1.9-fold), Major vault protein (1.8-fold), Bax (1.16-fold), and Cytochrome C (1.39-fold) indicate the activation of the intrinsic pathway. We also observed the differential expression of protein Complement C3 (3.3-fold), Destrin (−5.1-fold), Vimentin (−1.7-fold), Peroxiredoxin 4 (−1.6-fold), Fascin (−1.8-fold), Heme oxygenase-2 (−0.67-fold**$p < 0.0055$), Hsp27 (−0.57-fold**$p < 0.004$), and Hsp70 (−0.39-fold **$p < 0.001$), indicating reduced cell growth, cell migration, and metastasis. The upregulation of 40S ribosomal protein S9 (3-fold), 40S ribosomal protein S15 (4.2-fold), 40S ribosomal protein S18 (2.5-fold), and 60S ribosomal protein L22 (4.4-fold) implied the induction of translation machinery. These results reiterate the decisive role of 5-Aza-CdR in lung cancer treatment since it induces the epigenetic regulation of NY-ESO-1 antigen, inhibits cell proliferation, increases apoptosis, and decreases invasiveness.

* Corresponding author. Translational Cancer Research Facility, National Centre for Cancer Care and Research, Hamad Medical Corporation, Adjunct, Associate Professor, College of Health and Life Sciences (CHLS), Hamad Bin Khalifa University, Doha, Qatar.
E-mail address: sdermime@hamad.qa (S. Dermime).

https://doi.org/10.1016/j.ejphar.2023.175612
Received 29 November 2022; Received in revised form 16 February 2023; Accepted 17 February 2023
Available online 22 February 2023

1. Introduction

Lung cancer continues to be among the leading causes of cancer-related mortality in both men and women (Sung et al., 2021). Based on the morphology of the cells, lung cancer is divided into two categories; small cell lung cancer (SCLC), a highly malignant tumour which accounts for 15% of cases, the non–small cell lung cancer (NSCLC), which accounts for the majority (85%) of patients. Lung cancer therapy remains challenging despite the recent advancements in cancer cures (Thai et al., 2021) Immunotherapy, through the modulation of cancer-testis antigens (CTAs), is a revolutionizing cancer treatment that has evidently established benefits to therapeutic efficiency in lung cancer (Meng et al., 2021). The CTA NY-ESO-1 is a 180 amino acid long, 18 kDa cytoplasmic protein expressed exclusively in germ cells and not in normal adult tissues (Chen et al., 1997). Reports suggest that approximately 75% of cancer patients express NY-ESO-1 antigen during their illness in various tumours (Barrow et al., 2006). The NY-ESO-1 antigen is a potential candidate for immunotherapy since it is one of the best-characterized and most immunogenic CTA (Raza et al., 2020; Thomas et al., 2018), known for its ability to induce spontaneous antibody and T cell response in cancer patients (Merhi et al., 2018, 2020).

The native expression of the *NY-ESO-1* gene at the cellular level is often heterogeneous due to the epigenetic modifications that prevent the recruitment and sequential interaction of histone deacetylases, histone methyltransferase, DNA methyltransferases, and transcription factors *(Cartron* et al., *2013)*. Epigenetic modifications are critical regulators in oncogenesis that influence gene expression and other DNA-dependent processes without causing any change in the DNA coding sequence (Kanwal and Gupta, 2012). DNA methylation at the promoter CpG island region is among the major epigenetic modifications that cause gene silencing in cancer cells (Mahmood and Rabbani, 2019). This genetic regulation leads to the inactivation of the signaling pathways primarily related to cell cycle and apoptosis, and eventually transforms a normal cell into a malignant phenotype (Lu et al., 2020). Epigenetic dysregulation can be reversed using hypomethylating agents such as the 5-Aza-CdR (decitabine) drug which has been widely used to treat various cancers (Nervi et al., 2015). 5-Aza-CdR binds to DNA which consequently blocks DNA methyltransferase and decreases the DNA methylation process(Dan et al., 2019). Studies have observed that 5-Aza-CdR treatment reactivates the expression of silenced proapoptotic genes, which induce cancer cell death (Azad et al., 2013). 5-Aza-CdR has been shown to upregulate the expression of immunogenic CTAs through hypomethylation in their gene promoter region (Almstedt et al., 2010; Bao et al., 2011; Natsume et al., 2008).

In the present study, we investigated the decisive role of 5-Aza-CdR in the induction of the epigenetic regulation of NY-ESO-1 antigen, the inhibition of cell proliferation, the induction of apoptosis, and the ability to decrease the invasiveness of lung cancer cells.

Abbreviations

5 Aza-CdR	5-Aza-2′-deoxycytidine;
NSCLC	Non-Small Cell Lung Cancer
NY-ESO-1	New York Esophageal Squamous Cell Carcinoma-1
CTA	Cancer Testis Antigen
NSCLC	Non-small cell lung cancer
ELISA	Enzyme-Linked Immunosorbent Assay
RT-qPCR	Reverse Transcriptase Quantitative PCR
mRNA	Messenger RNA
cDNA	Complimentary DNA
GAPDH	Glyceraldehyde 3-phosphate dehydrogenase
RIPA	radioimmunoprecipitation assay
WST	Water-Soluble Tetrazolium Salt
RTCA	Real Time Cell Analyzer

2. Materials and methods

2.1. Chemicals

A vial containing 5 mg lyophilized powder of 5-Aza-CdR *(Sigma-Aldrich, USA)* was reconstituted with 20 mL sterile water *(Ampion, USA)* to get a 1 mM stock solution. The stock solution was stored away from light at 4 °C.

2.2. Cell lines and culture conditions

A panel of cancer cell lines; lung cancer - NCI–H1975 (epithelial cell line isolated from lung cells taken from a female with non–small cell lung cancer), HCC 827 (epithelial cell line isolated from lung cells taken from a female with non–small cell lung cancer); breast cancer - MDA-MB 468 (epithelial cell line isolated from a pleural effusion taken from a female with adenocarcinoma), MCF 7 (epithelial cell line isolated from breast tissue taken from a female with adenocarcinoma); prostate cancer - PC3 (epithelial cell line isolated from bone metastasis taken from a male with prostatic adenocarcinoma) and VCaP (epithelial cell line isolated from a male with prostatic cancer) were purchased from *ATCC (USA)* and propagated as per the recommended protocols.

2.3. Cellular ELISA

A panel of cancer cell lines; (NCI–H1975, HCC 827, MDA-MB 468, MCF 7, PC3 and VCaP) were seeded in a 96-well flat-bottom plate and cultured overnight under standard conditions. The cell culture medium (Roswell Park Memorial Institute (RPMI) 1640 (1X)) *(Gibco, UK)* was replaced with fresh media containing 10 μM of 5-Aza-CdR every 12 h for 48 h. After the 5-Aza-CdR treatment, the cells were cultured for 48 h in fresh media. The cells were then fixed in ice-cold ethanol *(VWR, France)*/acetone *(Sigma-Aldrich, USA)* mix (1:1) for 15 min on ice. Following phosphate-buffered saline (PBS)*(Gibco, UK)* wash twice, cells were blocked and permeabilized with 100 μL of PBS + 0.5% bovine serum albumin (BSA)*(Santa Cruz Biotechnology, USA)* + 0.5% Triton X-100 (*Sigma-Aldrich, USA*) for 2 h at 4 °C. Cells were then incubated with anti-NY-ESO-1 antibody (12D7) at 1:10,000 dilution in blocking buffer (3% BSA) *(Santa Cruz Biotechnology, USA)* for 2 h at 4 °C. Bound antibodies were detected after 1 h incubation at 4 °C with horseradish peroxidase (HRP)-labelled goat anti-human Fc secondary antibody (1:4000 dilution) (*Abcam, UK*). The plates were incubated with the substrate, 3,3′,5,5′-tetramethylbenzidine (TMB) *(Sigma Aldrich, USA)* for 5 min, after which the reaction was stopped using 1N Hydrochloric Acid (HCL) *(Sigma Aldrich, USA)*. The plates were read at 450 nm using an ELISA reader *(Bio-Rad Laboratories, USA)* (Gupta et al., 2013).

2.4. DNA and RNA isolation

The NCI–H1975 cell line (7.5×10^5) was seeded and allowed to attach overnight in a T75 culture flask. Then the cell culture medium (RPMI 1640 (1X)) was replaced four times with fresh media containing 5-Aza-CdR (0 and 10 μM) every 12 h. After 5-Aza-CdR treatment, the cells were cultured for 48 h in fresh media. DNA and RNA were extracted using RNA/DNA/Protein Purification Plus Kit *(Norgen Biotek Corp, Canada)* as per the manufacturer's protocol. The cells were lysed with SKP lysis buffer and incubated at 55 °C for 10 min. Cell lysates were collected by centrifugation at 14,000 rpm for 5 min at 4 °C. DNA was separated from the lysates using a DNA extraction column. The flow-through from the DNA column was further used for RNA purification using the RNA extraction column. RNA quantification was performed using Nanodrop 2000c *(Thermo Scientific, USA)*.

2.5. CpG methylation assay

The CpG methylation analysis was performed as described earlier by Sasidharan Nair V et al. (Sasidharan Nair et al., 2018). Bisulfite treatment of the extracted DNA was performed using EZ DNA Methylation Kit *(Zymo Research, USA)*. The bisulfite-treated DNA was then subjected to Polymerase Chain Reaction (PCR) for amplifying the *NY-ESO-1* CPG islands using hot start TaKaRa Taq DNA polymerase *(TaKaRa Bio, Japan)*. PCR primers were designed using MethPrimer software *(*http://www.urogene.org/methprimer/index1.html*)* (Li and Dahiya, 2002). The primer sequences are available in the supplementary file (Supplement 1). The amplified PCR products were cloned into the pGemT-easy vector as per the manufacturer's instructions *(Promega, USA)*. Ligated products were transformed into JM109 competent cells (*Promega, USA*), and positive clones were selected using Amp resistant gene. The plasmid DNA was isolated using Wizard® Plus SV Minipreps DNA Purification System *(Promega, USA)* and sequenced using M13-specific primers *(Promega, USA)*.

2.6. RT-qPCR assay

Superscript IV reverse transcription kit *(Invitrogen, Thermo Fisher Scientific, Lithuania)* was used to synthesize cDNA from total RNA (2 μg) using random hexamers, and the experiment was performed according to the manufacturer's instructions. This cDNA (100 ng) was used for the quantitative polymerase chain reaction (qPCR) in a 20 μL reaction volume containing TaqMan reaction mix and assay buffer *(Applied Biosystems, USA)*. The internal control Glyceraldehyde 3-phosphate dehydrogenase (GAPDH) was used to normalize the CT values of the *NY-ESO*-1 mRNA target. Then 2–ΔΔCt method was applied to calculate fold changes in the treated sample compared to the untreated sample.

2.7. Cell viability

The NCI–H1975 cell line (5000 cells/well) was seeded in a 96-well, flat bottom plate and treated with different concentrations of 5-Aza-CdR (0, 1 μM, 2.5 μM, 5 μM, 7.5 μM, 10 μM, 15 μM, and 20 μM) as explained above. After treatment, the medium (RPMI 1640 (1X)) was replaced with 5-Aza-CdR-free fresh medium, and the cells were further cultured for 48 h and 72 h. The cytotoxicity was then analysed using WST Kit *(Roche Applied Science, Germany)* as per the manufacturer's instructions. WST reagent was added to the well in 1:10 final dilution, and the plate was incubated for 1 h. Absorbance was measured at 450 nm. Cell viability percentage (metabolic activity) was calculated using the following formula: (mean optical density (OD) of the experiment samples/mean OD of the untreated sample) × 100.

2.8. Cell proliferation analysis

For the Real-Time Cell Analysis (RTCA) assay, the NCI–H1975 cell line (5000 cells/well) was seeded in E-plate 16 *(xCELLigence, Roche, USA)* and treated with different concentrations (0, 2.5 μM, 5 μM, 7.5 μM, and 10 μM) of 5-Aza-CdR as described above. The electrical impedance recorded as cell index measured cell viability with 5-Aza-CdR-treatment.

2.9. Morphological changes

To analyse the cellular morphology after 5-Aza-CdR treatment, the NCI–H1975 cell line was seeded in a 6-well plate at 100,000 cells/well density. 5-Aza-CdR treatment was performed as described above. Images of untreated and 5-Aza-CdR treated (10 μM) cells were captured under a microscope *(Nikon ECLIPSE, Japan)* at 20× magnification.

2.10. Proteomics assay

2.10.1. Experimental design

The NCI–H1975 cell line (7.5×10^5) was cultured in a T75 flask for proteomics analysis. 5-Aza-CdR treatment was performed as explained above. After 48 h treatment, all the cells were collected and centrifuged. The pellet was dissolved in radioimmunoprecipitation assay (RIPA) buffer (*Sigma-Aldrich, USA)* containing protease-phosphatase inhibitor cocktail (*Roche Applied Science, Germany*). The total cell lysate was obtained after centrifugation at 14,000 g for 15 min at 4 °C. Protein concentration was quantified using the Rapid Gold BCA Protein assay kit *(Pierce™, Thermo Scientific, USA)*.

2.10.2. Sample preparation

50 μg of extracted protein was digested with sequencing grade modified trypsin (12.5 ng/L) *(Promega, USA)* prepared in ammonium bicarbonate (ABC) buffer (*Sigma-Aldrich, USA)* at 37 °C overnight. The peptides were cleaned and desalinated in the Stage tip. Peptides were further concentrated by vacuum centrifugation and reconstituted in 10 μL of 5% formic acid *(Sigma-Aldrich, USA)* (Rappsilber et al., 2007).

2.10.3. Liquid chromatography-tandem Mass Spectrometry (LC-MS/MS)

Mass Spectrometry was performed on a quadrupole-time-of-flight mass spectrometer *(MS-QTOF 6550, Agilent Technologies, USA)* coupled to a nano-liquid chromatography system *(Agilent Technologies, USA)*. The concentrated peptides were separated on a C18 column (15 cm long with an inner diameter of 75 μm) (*Zorbax 300SB-C18, Agilent Technologies, USA)* using a gradient of buffer A (Ultrapure water, *(Riedel-de Haen, Honeywell, Germany)*, 1% formic acid and buffer B (Acetonitrile (*Riedel-de Haen, Honeywell, Germany)*, 1% formic acid at a flow rate of 300 nL min-1. The chromatographic gradient was set to provide a linear increase from 2% of buffer B to 80% in 110 min and the total run time was 120 min. MS data was acquired in data-dependent mode, dynamically choosing the top ten most abundant precursor ions from the survey scan (400–1800 m/z) for fragmentation and MS/MS analysis. Precursors with a charged state of +1 were rejected, and the dynamic exclusion duration was set as 25 s. The MS raw data is available in the supplementary file (Supplement 2).

2.10.4. MS data processing and analysis

MS raw data was processed using MaxQuant software version 1.5.5.1 according to the standard workflow (Tyanova et al., 2016) with the built-in search engine Andromeda (Cox et al., 2011). Proteins were identified by analyzing the Uniprot human reference proteome (July 2019) database. Carbamidomethylation of cysteines was destined as a fixed modification, while protein N-terminal acetylation and methionine oxidation were defined as variable modifications for peptide search. The false discovery rates (FDR) for peptide and protein identifications were set to 1%. A maximum of two missed cleavages were allowed for tryptic digestion. The MaxLFQ label-free quantitation method with retention time alignment and match-between-runs feature in MaxQuant was applied to extract the maximum possible quantification information. Protein abundance was calculated based on normalized spectral intensity (LFQ intensity). Data analysis was performed using the freely available software Perseus (version 1.6.2.3) *(*https://maxquant.net/perseus/*)*. LFQ intensities from the MaxQuant analysis were imported, transformed by log2, and the missing LFQ intensity values were imputed with the value of the lowest LFQ intensity from the normal distribution (width = 0.3, downshift = 1.8). Protein quantification and statistical significance were calculated using the two-tailed Student's t-test with a permutation-based FDR of 5% to truncate all test results. P value of <0.05 with fold change ratio >2 or <1.5 indicated significant changes in protein abundance. The gene ontology (GO) annotation of the significantly dysregulated proteins, carried out using FunRich (version 3.1.3) *(http://www.funrich.org/)* functional enrichment analysis tool (Pathan et al., 2015), resulted in identifying the distribution of

enriched proteins involved in various domains such as cellular components, biological process, molecular functions, and biological pathways.

2.11. Protein array analysis

The NCI–H1975 cell line (7.5×10^5 cells) was seeded in a T75 culture flask, and the treatment was performed as described above. After 48 h of treatment, the cell lysates were prepared. According to the manufacturer's instructions, the dysregulation of apoptosis-related proteins was analysed using Proteome profiler Human apoptosis array (*R&D Systems, USA*) kits. Protein concentration was measured by the Rapid Gold BCA Protein assay kit. After successive blocking, pre-coated array membranes were incubated with untreated and treated proteins at 4 °C overnight. After consecutive washes, the array membranes were washed and incubated with the detection antibody cocktail for 1.5 h at room temperature. After a thorough wash, the membranes were incubated with diluted streptavidin-HRP for 30 min at room temperature. The protein dots were spotted by adding a Chemi Reagent Mixture (supplied with the kit). The dots were visualized, and images were captured by a ChemiDoc™ MP imaging system (*Bio-Rad, USA*). Densitometric analysis was done to quantify the strength of the spot using Image J software. The pixel density of each duplicated dot in the array was averaged and normalized against the reference spots, and the relative levels were expressed as mean pixel intensity. The identity and coordinates of all the antibodies orientated on arrays are described in the Supplementary Material (Supplement 3).

3. Results

3.1. Effects of 5-aza-CdR treatment on NY-ESO-1 expression in cancer cells

We first examined the up-regulation of the NY-ESO-1 protein in a panel of cancer cell lines (lung cancer: NCI–H1975, HCC 827; breast cancer: MCF 7, MDA-MB 468; and prostate cancer: PC3 and VCaP) treated with 10 μM of 5-Aza-CdR. Cellular ELISA identified that the untreated cells did not show any basal level of NY-ESO-1 protein expression. However, 10 μM of 5-Aza-CdR treatment induced the expression of NY-ESO-1 in all tested cell lines with the exception of MDA-MB 468 and VCaP. The NY-ESO-1 induction was significantly higher in NCI–H1975 (**$p < 0.0097$), PC3 (**$p < 0.0426$), MCF7 (**$p < 0.0033$) and HCC827 (*$p < 0.013$) (Fig. 1A). The lung cancer cell line NCI–H1975, which showed the highest NY-ESO-1 induction was selected for further analysis. We then validated the cellular ELISA results using RT-qPCR. RT-qPCR results showed a significant increase in the *NY-ESO*-1 mRNA expression (128-fold increase, *$p < 0.0500$) after the

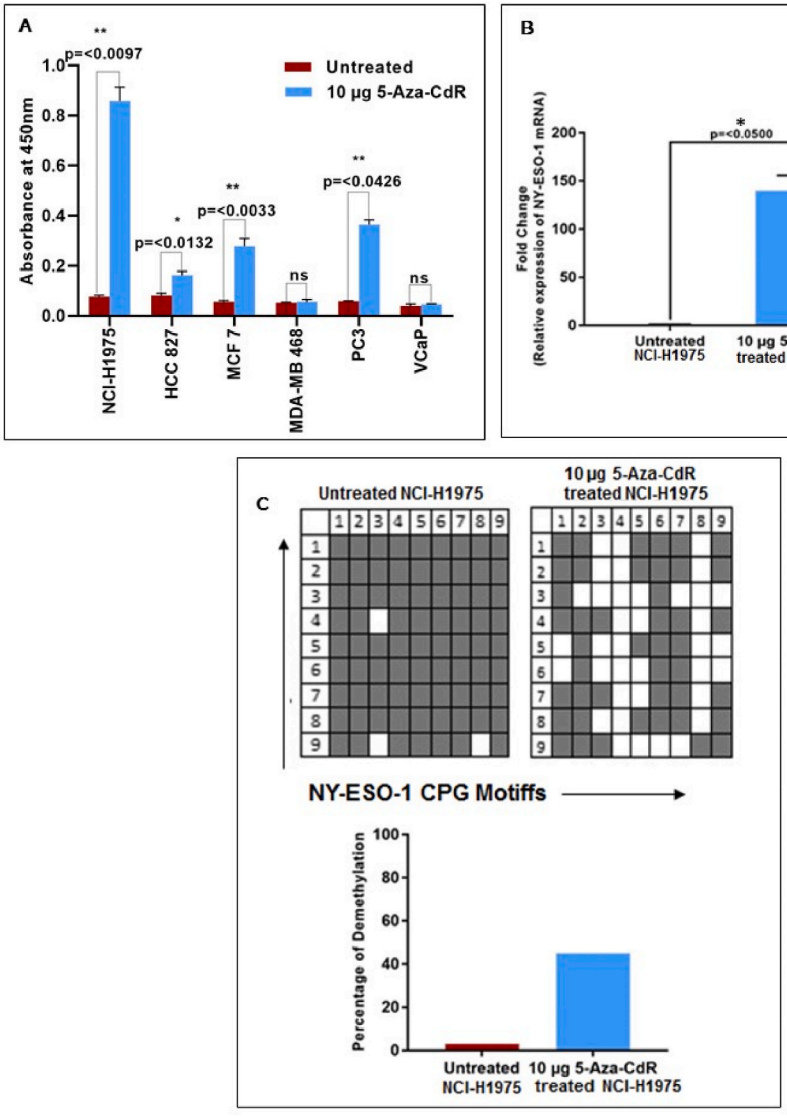

Fig. 1. Treatment with 5-Aza-CdR induces the expression of NY-ESO-1 tumour antigen. (A) We treated a panel of cancer cell lines, lung cancer (NCI–H1975, HCC 827), breast cancer (MDA-MB 468, MCF 7), and prostate cancer (PC3 and VCaP) with 10 μM of 5-Aza-CdR. Cellular ELISA results showed significant induction of NY-ESO-1 protein in NCI–H1975 (**$p < 0.0097$) cell line, which was selected for our further studies. (B) The mRNA expression levels of *NY-ESO-1* gene in 10 μM 5-Aza-CdR treated and untreated NCI–H1975 cell line was analysed by qRT-PCR, and results showed a significant increase in the *NY-ESO*-1 mRNA expression (128-fold increase, *$p < 0.0500$) compared with the untreated cells. These data are from duplicate experiments and presented as mean ± SD. (C) Our bisulfite sequencing results indicated 10 μM of 5-Aza-CdR treatment induced 45.6% demethylation at the *NY-ESO-1*gene promoter region in NCI–H1975 cell line.

treatment of NCI–H1975 with 10 μM of 5-Aza-CdR (Fig. 1B).

The bisulfite sequencing data showed that only 3% of the CpG islands of the *NY-ESO-1* gene promoter region were demethylated in untreated NCI–H1975 cells, while 10 μM 5-Aza-CdR treatment enhanced the demethylation efficiency by 45.6% (Fig. 1C), thus, reinstating our results with cellular ELISA and RT-qPCR.

3.2. Cytotoxic analysis of 5-aza-CdR

Cytotoxicity of 5-Aza-CdR was tested using WST and RTCA analysis. The NCI–H1975 cell line was treated with incrementing concentrations of 5-Aza-CdR to measure the IC50 value. After 48 h of treatment, a drastic reduction of cell viability was observed in the 5-Aza-CdR treated cells compared with the untreated cells. Cell viability decreased with increasing concentrations, and no further changes were observed in the two higher concentrations tested, 15 μM and 20 μM (47%) (Fig. 2A). The IC50 value of 5-Aza-CdR for NCI–H1975 was determined to be 11.20 μM. xCELLigence RTCA was used to understand the real-time cell proliferation of NCI–H1975 cell line in response to 5-Aza-CdR. RTCA results showed that 5-Aza-CdR induces a significant dose dependent inhibition of cell proliferation in NCI–H1975 cell line (Fig. 2B) in concordance with the WST analysis. Additionally, we found that 5-Aza-CdR (10 μM) treatment induces morphological changes in the NCI–H1975 cell line; displaying swollen, stretched, loosely distributed particulate cells (Fig. 2C).

3.3. Proteomic profiling of 5-aza-CdR treated NCI–H1975 cells

We performed a label-free quantitative shotgun proteomics approach to gain insights into the transcriptomic changes induced by the 5-Aza-CdR in NCI–H1975 cell line. We observed 347 proteins in untreated and 328 in 5-Aza-CdR treated cells (Fig. 3A). We identified 259 common

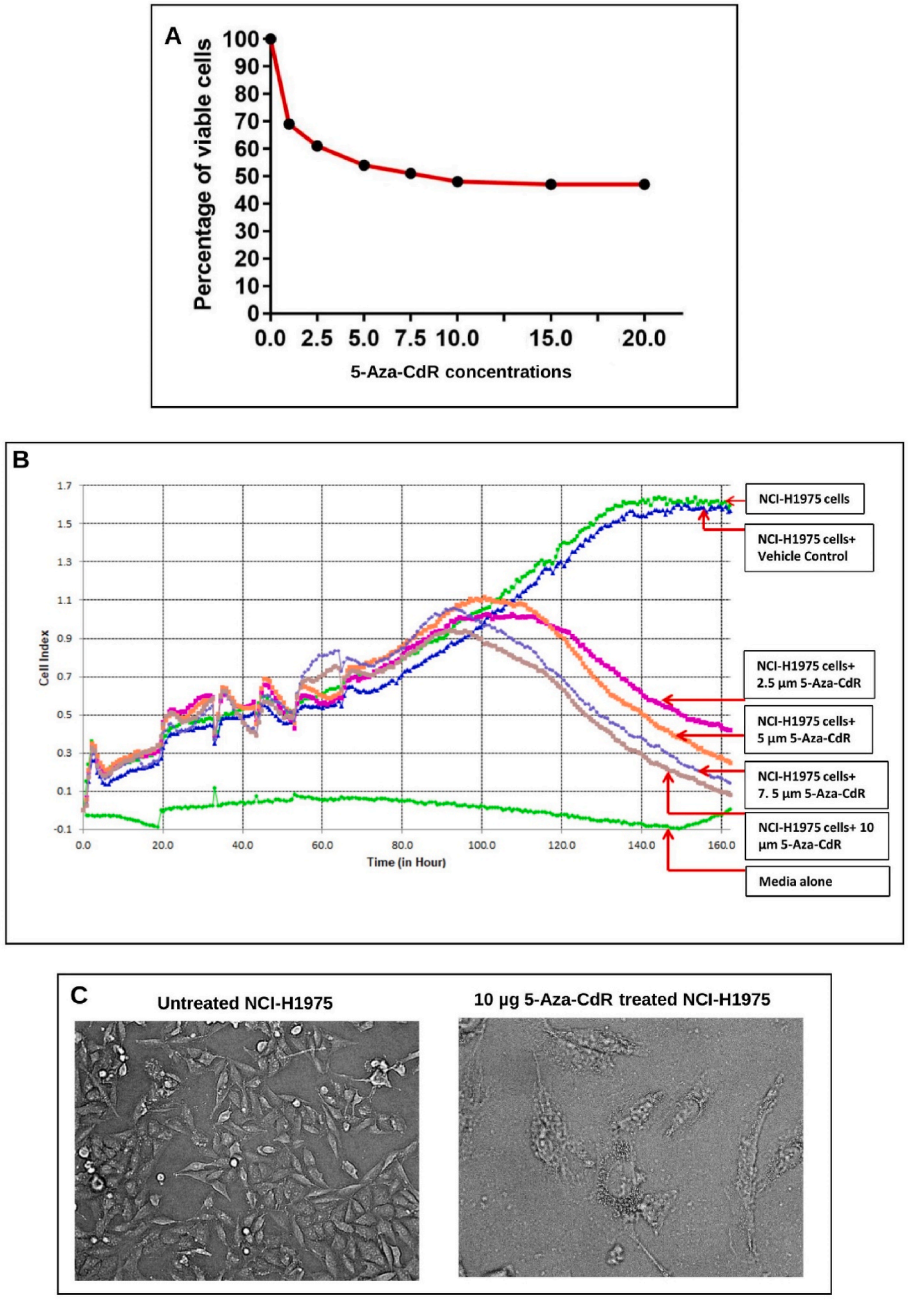

Fig. 2. Cytotoxic analysis of 5-Aza-CdR in NCI–H1975 cell line. (A) NCI–H1975 cell line was treated with incrementing concentrations of 5-Aza-CdR and cytotoxicity was analysed using WST assay. Results indicated a drastic reduction of cell viability with increasing concentrations of 5-Aza-CdR, and no further changes were observed in the two higher concentrations tested, 15 μM and 20 μM (47%). (B) xCELLigence Real time cell proliferation (cell index) analysis of NCI–H1975 cell line in response to 5-Aza-CdR treatment showed a significant dose and time-dependent inhibition of cell proliferation. (C) 5-Aza-CdR treatment resulted in significant morphological changes in NCI–H1975 cell line such as swelling, stretching, and intracellular particles. Images were captured using bright-field microscope (Olympus IX51, objective 20x).

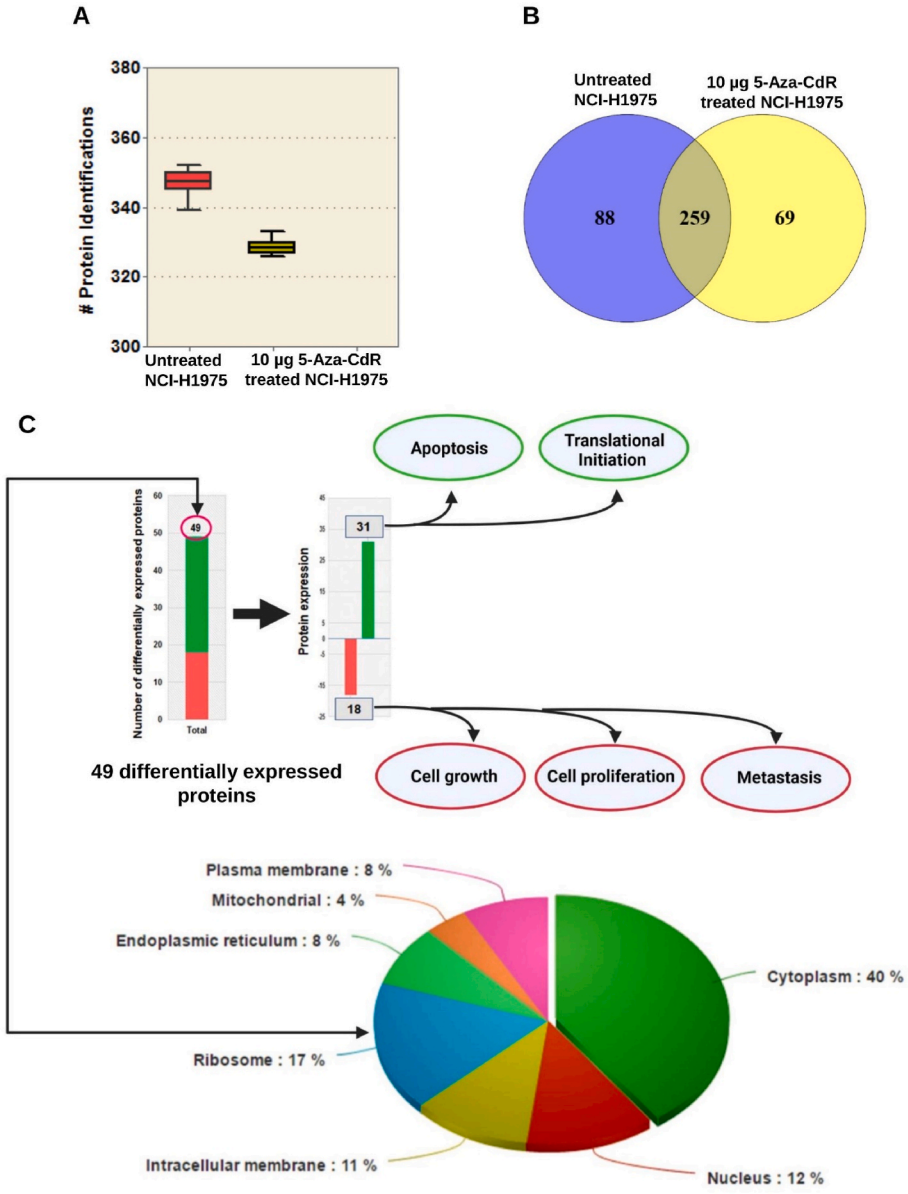

Fig. 3. Proteomic data interpretation and visualization. (A) and (B): Label-free quantitative shotgun proteomics approach was used to study the transcriptomic changes induced by 5-Aza-CdR in NCI–H1975 cell line. We identified 347 proteins in untreated and 328 in 5-Aza-CdR treated cells in which, 259 proteins were observed as common proteins between untreated and treated samples. The spectral intensity of relative protein abundance was calculated using a label-free quantification approach (MaxQuant label-free algorithm (LFQ). With FDR <0.05 as the *t*-test significance threshold and fold-change >2 or <1.5 as the differential abundance threshold, we found 49 proteins to be significantly dysregulated; 31 of these were found to be upregulated while 18 proteins were downregulated. (C) Functional annotation of dysregulated proteins results revealed that dysregulated proteins were localized mainly in the cytoplasm (40%), ribosome (17%), nucleus (12%), and intracellular membrane (11%). The functional analysis further revealed that differentially expressed proteins are responsible to induced apoptosis and translational initiation and downregulated the cell growth, proliferation, and metastasis.

proteins (Fig. 3B) between untreated and treated samples. The spectral intensity of relative protein abundance was calculated using a label-free quantification approach (MaxQuant label-free algorithm (LFQ). With FDR <0.05 as the *t*-test significance threshold and fold-change >2 or <1.5 as the differential abundance threshold, we found 49 proteins to be significantly dysregulated; 31 of these were found to be upregulated (Table 1), while 18 proteins were downregulated (Table 2).

3.4. Functional annotation of dysregulated proteins

Functional annotation of dysregulated proteins was analysed using the FunRich tool. The results revealed that dysregulated proteins with 5-Aza-CdR treatment were localized mainly in the cytoplasm (40%), ribosome (17%), nucleus (12%), and intracellular membrane (11%) (Fig. 3C). The functional analysis of differentially expressed proteins revealed that 5-Aza-CdR treatment upregulated the expression of the proteins related to apoptosis and translational initiation, and downregulated the proteins associated with cell growth, proliferation, and metastasis (Fig. 3C). The intrinsic apoptosis pathway-related proteins, such as Voltage-dependent anion-selective channel protein 1 (1.9-fold), Major vault protein (1.8-fold), and Cytochrome C (2.5-fold), were found to be upregulated (Tables 1 and 2). Various proteins related to translation machinery such as 40S ribosomal protein S9 (3-fold), 40S ribosomal protein S15 (4.2-fold), 40S ribosomal protein S18 (2.5-fold), and 60S ribosomal protein L22 (4.4-fold) were found to be upregulated. In addition, cell growth, migration, and metastasis related proteins were differentially expressed. Protein Complement C3 (3.3-fold) was found to be upregulated, whereas Destrin (−5.1-fold), Vimentin (−1.7-fold), Peroxiredoxin 4 (−1.6-fold), and Fascin (−1.8-fold) were found to be significantly downregulated (Tables 1 and 2).

3.5. Functional analysis of differentially expressed proteins

Functional analysis of differentially expressed proteins was further validated using Proteome profiler Human apoptosis array (R&D Systems) (Fig. 4A). The protein array data showed significant downregulation of anti-apoptotic proteins Bcl-2 (0.60-fold **$p < 0.002$), cIAP1 (0.49-fold **$p < 0.015$), Survivin (0.71-fold***$p < 0.047$) and upregulation of pro-apoptotic protein Bax (1.16-fold) (Fig. 4B). The apoptosis executor protein, Cleaved Caspase-3 (2.2-fold), was

Table 1
Proteins upregulated by 5-Aza-CdR treatment in NCI–H1975 cell line identified by label-free shotgun proteomics approach.

Uniport ID	Protein Name	Fold Change
P26373	60S ribosomal protein L13	1.9
P62081	40S ribosomal protein S7	2.5
P32969	60S ribosomal protein L9	2.1
Q00839	Heterogeneous nuclear ribonucleoprotein U	2.4
Q04637-9	Isoform 9 of Eukaryotic translation initiation factor 4 gamma 1	2.3
K7ELC2	40S ribosomal protein S15	4.2
P62269	40S ribosomal protein S18	2.5
P35268	60S ribosomal protein L22	4.4
A0A024R4M0	40S ribosomal protein S9	3.0
P62314	Small nuclear ribonucleoprotein SM D1	2.4
E5KLJ5	Dynamin-like 120 kDa protein, mitochondrial	1.9
P62191	26S proteasome regulatory subunit 4	1.5
O00629	Importin subunit alpha-3	2.3
Q9Y5B9	FACT complex subunit SPT16	1.7
H7BZJ3	Protein disulfide –isomerase A3 (Fragment)	2.5
P17655	Calpain-2 catalytic subunit	3.2
Q9Y230	RuvB-like 2	4.7
P16402	Histone H1.3	2.0
Q99436	Proteasome subunit beta type-7	1.7
P21796	Voltage- dependent anion- selective channel protein 1	1.9
Q8WUM4-2	Isoform 2 of programmed cell death6-interacting protein	2.1
P99999	Cytochrome *c*	2.5
Q99623	Prohibitin-2	1.8
P35235	Prohibitin	1.5
P01024	Complement C3	3.3
U3KQK0	Histone H2B	2.1
P55060	Exportin-2	2.8
O00410-3	Isoform 3 of importin-5	1.5
Q14764	Major vault protein	1.8
Q15084-2	Isoform 2 of Protein disulphide-isomerase A6	2.2
Q13200	26S proteasome non- ATPase regulatory subunit 2	1.5

Table 2
Proteins downregulated by 5-Aza-CdR treatment in NCI–H1975 cell line identified by label-free shotgun proteomics approach.

Uniport ID	Protein Name	Fold Change
P37802-2	Isoform 2 of Transgelin-2	−1.9
P08670	Vimentin	−1.7
P09382	Galectin-1	−2.2
P14625	Endoplasmin	−2.6
P07339	Cathepsin D	−1.9
Q13263	Transcription intermediary factor 1-beta	−2.4
Q16658	Fascin	−1.8
P10599	Thioredoxin	−2.5
P25398	40S ribosomal protein S12	−3.2
P60981	Destrin	−5.1
Q99497	Protein DJ-1	−3.1
P05455	Lupus La protein	−3.6
P35221-2	Isoform space2 of Catenin alpha-1	−2.2
P07355-2	Isoform 2 Annexin A2	−4.4
Q13162	Peroxiredoxin-4	−1.6
Q14152	Eukaryotic translation-initiation factor 3 subunit A	−2
P20700	Lamin-B1	−5
P27361	Mitogen-activated protein kinase 3	−2

upregulated (Fig. 4C). Moreover intrinsic apoptotic protein Cytochrome C (1.3-fold) and extrinsic pathway proteins TRAIL (2.04-fold *$p < 0.0117$) and FAS (2.1-fold) were upregulated while the cell survival proteins HMOX2 (−0.68-fold), HSP27 (−0.52-fold), and HSP70 (−0.40-fold **$p < 0.010$) were downregulated (Fig. 4D and E).

4. Discussion

Dysregulated epigenetic modifications are common in lung cancers but have been shown to be reversed using demethylating agents such as 5-Aza-CdR. 5-Aza-CdR has been proven effective in NSCLC treatment as a monotherapy or combination with immunotherapy but has not been fully exploited (Juergens et al., 2011). The native expression of the *NY-ESO-1* gene at a cellular level is often heterogeneous *due to the methylation* of the CPG islands in the *NY-ESO-1* gene promoter region (Aung et al., 2014; Sugita et al., 2004; Velazquez et al., 2007). 5-Aza-CdR is known to induce gene expression through DNA demethylation following DNA methyltransferase sequestration. It has been demonstrated that 5-Aza-CdR was able to induce/upregulate the NY-ESO-1 antigen in the NCI–H1975 lung cancer cell line (Chüeh et al., 2017). We investigated in the present study the epigenetic regulation of the NY-ESO-1 antigen and the molecular mechanism of apoptosis induced by 5-Aza-CdR in the NCI–H1975 non-small lung cancer cell line. In this study, we determined that 5-Aza-CdR treatment was able to induce NY-ESO-1 expression and activate the pathways that promote cytotoxicity in the NCI–H1975 lung cancer cell line. Initially we confirmed the ability of 5-Aza-CdR to significantly induces/upregulates the expression of the NY-ESO-1 antigen in NCI–H1975 cells through demethylation of CpG islands of the promoter region of the *NY-ESO-1* gene as reported earlier in other cancers (Almstedt et al., 2010; Bao et al., 2011; Natsume et al., 2008). Then we investigated the anti-cancer effects accompanied with the demethylating effect of 5-Aza-CdR in NCI–H1975 cells. There was a significant inhibition of cell proliferation and activation of apoptosis through both intrinsic and extrinsic pathways. It has been demonstrated that death ligand and receptor binding can trigger the extrinsic apoptotic pathway in lung cancer (Viktorsson and Lewensohn, 2007). The upregulation of the death receptors FAS (2.1-fold) and TRAILs (2.04-fold *$p < 0.011$) demonstrated in our study may indicate activation of the extrinsic apoptotic pathway through such a mechanism. This recruits a series of downstream factors, including Caspase-3. We have shown that the intrinsic apoptosis pathway, initiated by DNA damage in the 5-Aza-CdR treated cells, leads to caspase 3 cleavage which causes the proteolytic cleavage of the PARP protein in 2 fragments: an 89 kDa C-terminal fragment with reduced catalytic activity and a 24 kDa N-terminal peptide, which retains the DNA binding domains. The PARP protein loses the nick-sensor function after its cleavage which prevents DNA repair and activates the intrinsic apoptotic pathway (Viktorsson and Lewensohn, 2007). The intrinsic signaling pathways rely on mitochondria-initiated events producing intracellular signals that act directly on targets within the cell (Elmore, 2007; Wang and Youle, 2009). Interestingly, upregulation of the voltage-dependent anion-selective channel protein 1 (VDAC1), the major vault protein (MVP), and the cytochrome C was demonstrated in our study. VDAC1 is located in the outer mitochondrial membrane and is known to play a crucial role in mitochondrial-mediated apoptosis through the release of Cytochrome C (Shoshan-Barmatz et al., 2017). VDAC1 is highly Ca2+-permeable, and the enhanced expression of VDAC1 modulates Ca2+ access to the mitochondrial intermembrane space. This increase in Ca2+ augments VDAC1 oligomerization, followed by Cytochrome C release (Shoshan-Barmatz et al., 2017). Alternatively, the upregulation of MVP can induce cell apoptosis by inhibiting the STAT 3 pathway (Bai et al., 2019). This inhibition, in turn, reduces the expression of anti-apoptotic proteins Bcl-2 and Survivin resulting in increased mitochondrial inner membrane permeability and Cytochrome C release (Weerasinghe et al., 2007). It is important to mention that these 2 proteins were additionally shown to be significantly reduced in our 5-Aza-CdR-treated cells (Fig. 4). We have demonstrated a significant upregulation of the Bax protein which is a member of the Bcl-2 family and core regulator of the intrinsic apoptotic pathway. An increase in Bax protein promotes mitochondrial outer membrane permeabilization. Consequently, this leads to the Cytochrome C release into the cytosol where it engages with the apoptotic protease activating factor-1 (APAF1) and forms the apoptosome, which further triggers downstream effector caspases such as Caspase-9 and Caspase-3 (Lucken-Ardjomande and Martinou, 2005) (Fig. 5).

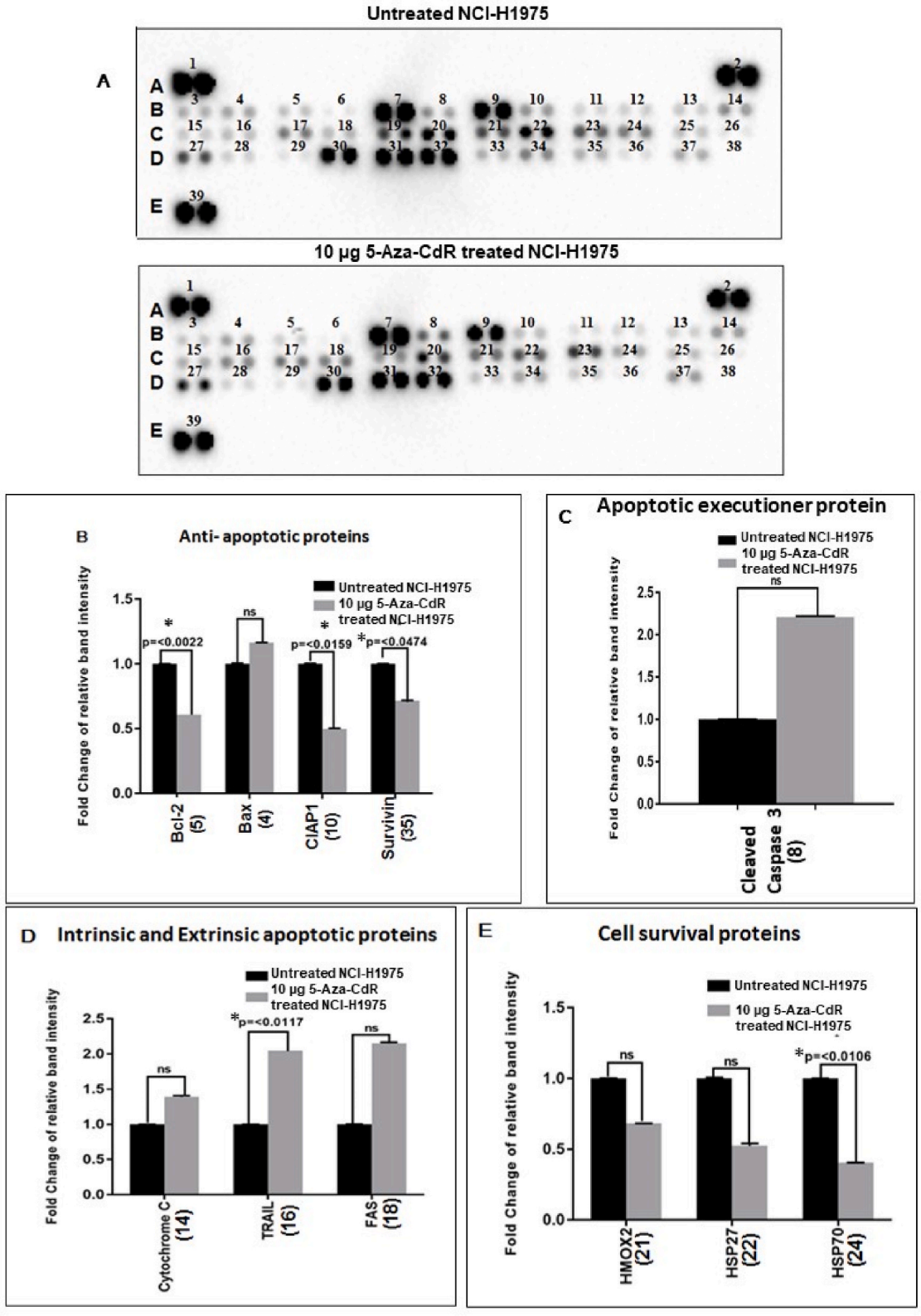

Fig. 4. Apoptotic pathways enriched by 5-Aza-CdR in NCI–H1975 cell line and their validation. (A) Apoptotic pathways enriched by 5-Aza-CdR treatment in NCI–H1975 cell line was validated using proteome profiler human apoptosis array (R&D Systems). (B) The protein array data showed significant downregulation of anti-apoptotic proteins Bcl-2 (−0.60-fold *p < 0.002), cIAP1 (−0.49-fold *p < 0.0159), Survivin (−0.71-fold *p < 0.0474) and upregulation of pro-apoptotic protein Bax (1.16-fold). (C) The apoptosis executor protein, Cleaved Caspase-3 (2.2-fold), was upregulated. (D) Also, intrinsic apoptotic protein Cytochrome C (1.3-fold) and extrinsic pathway proteins TRAIL (2.04-fold *p < 0.011) and FAS (2.1-fold) were upregulated. (D) The cell survival proteins HMOX2 (−0.682-fold), HSP27 (−0.52-fold), and HSP70 (−0.404-fold *p < 0.0106) were downregulated.

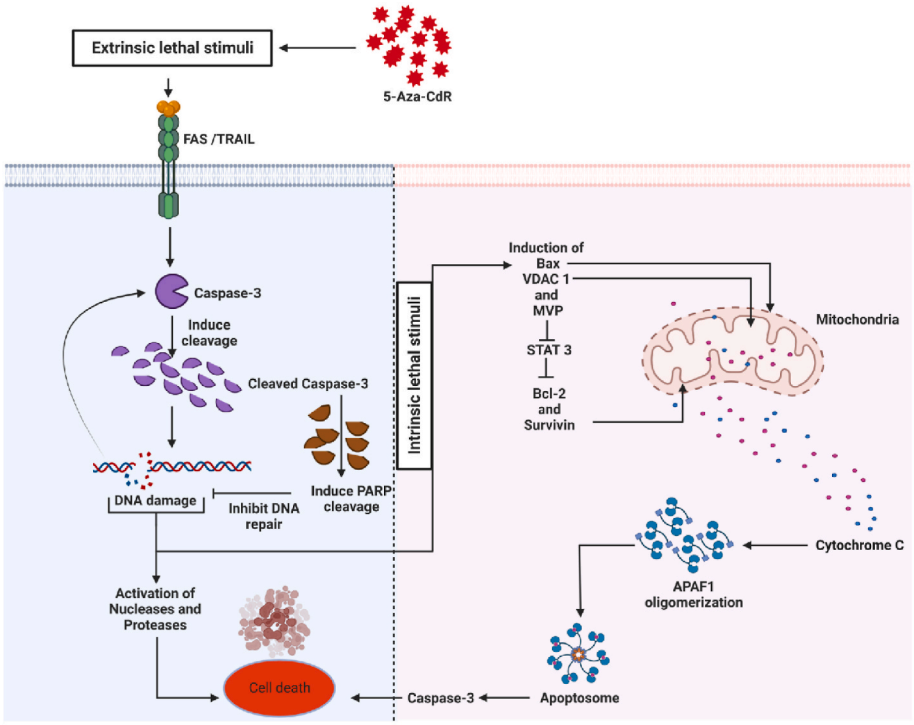

Fig. 5. Apoptotic mechanism induced by 5-Aza-CdR treatment in NCI–H1975 cell line. 5-Aza-CdR treatment induced apoptosis in NCI–H1975 cell line through extrinsic and intrinsic pathways. 5-Aza-CdR treatment induced extrinsic pathway by upregulates the death receptors (FAS and TRAILs) and this will recruit a series of downstream factors that induce Caspase 3 cleavage. Cleaved caspase 3 will cause PARP cleavage and this inhibits the DNA repair machinery, initiating DNA damage and eventually cell death. Increased DNA damage will be an intrinsic lethal stimulus that instigates several mitochondrial apoptotic events. Enhanced expression of VDAC1 modulates Ca2+ access to the mitochondrial intermembrane space. This increase in Ca2+ augments VDAC1 oligomerization, followed by Cytochrome C release. An increase in Bax protein promotes mitochondrial outer membrane permeabilization which also leads to the Cytochrome C release. The upregulation of MVP protein can induce cell apoptosis by inhibiting the STAT 3 pathway, thus reducing the expression of anti-apoptotic proteins Bcl-2 and Survivin. This again results in increased mitochondrial inner membrane permeability and Cytochrome C release. Cytochrome C release into the cytosol engages with the apoptotic protease activating factor-1 (APAF1) and forms the apoptosome, which further triggers downstream effector caspases such as Caspase-9 and Caspase-3 ultimately leading to cell death.

Furthermore, we have identified, in the present study, that several proteins (related to cell growth, migration, and metastasis) were differentially expressed. The complement component 3 (C3) was found to be upregulated, whereas Destrin, Vimentin, Peroxiredoxin 4, and Fascin were reduced in the 5-Aza-CdR-treated cells. C3 is an essential protein of the complement system, expressed in numerous cancer tissues, and has been studied extensively for its role in tumour progression. C3 expression increased 3.3-fold in the 5-Aza-CdR treated cells, and the indicated accumulation could be attributed to the prevention of the cleavage of C3 into its active fragments (C3a and C3b). The inhibition of the complement pathway at this level efficiently blocks cell proliferation and migration capability (Kleczko et al., 2019; Revel et al., 2020). Earlier studies have reported the prognostic value of C3 in NSCLC, where low C3 expression has been associated with poor prognosis (Lin et al., 2014). However, further research is required to probe the effect of 5-Aza-CdR in the complementary pathway system. Destrin is a small actin-binding protein that remodels the actin cytoskeleton vital for cancer cell migration and invasion (Zhang et al., 2021). Silencing Destrin in pancreatic cancer cells decreased invasiveness and migration, which reduced the proliferation of these cells (Klose et al., 2012). Fascin is an actin-binding protein that regulates cytoskeletal structures to maintain cell adhesion and coordinates motility and invasion through its interaction with signaling pathways (Liu et al., 2021). Downregulation of Fascin has been shown to reduce cell migration activity (Al-Alwan et al., 2011). Vimentin is the member of intermediate filament (IF) family of proteins responsible for maintaining cellular integrity and providing resistance to stress. Vimentin's overexpression in cancer correlates well with increased tumour growth, invasion, and poor prognosis (Berr et al., 2021; Satelli and Li, 2011). Peroxiredoxin 4 is preferentially expressed in lung cancer cells, and its reduced expression decreases the cell invasion capability (Jiang et al., 2014; Nicolussi et al., 2017). Thus, downregulation of Destrin, Vimentin, Peroxiredoxin 4, and Fascin by 5-Aza-CdR treatment observed in our study may lead to the suppression of tumour growth and invasion.

Using the protein array technology, we have demonstrated the downregulation of several heat shock proteins (Heme oxygenase-2, Hsp27 and Hsp70) known to be essential for cell survival. Downregulation of these proteins after 5-Aza-CdR treatment may decrease cell proliferation and migration capabilities of the cancer cells (Wu et al., 2017).Nonetheless, 5-Aza-CdR treatment was able to upregulate various proteins related to translation machinery, such as 40S ribosomal protein S9, 40S ribosomal protein S15, 40S ribosomal protein S18, and 60S ribosomal protein L22. The demethylating effect of 5-Aza-CdR may induce the expression of many genes that gradually enhance the cell translation machinery (Van Rechem et al., 2015). Collectively, our results demonstrated the mechanisms of the anti-cancer effect of 5-Aza-CdR treatment in the NCI–H1975 lung cancer cell line. These are in accordance with previous studies showing that 5-Aza-CdR treatment, in other cancers, was able to inhibit cell proliferation, increase apoptosis, and decrease the ability of cell invasion (Carbajo-García et al., 2021; Chen et al., 2019; Hassler et al., 2012; Liu et al., 2012).

To the best of our knowledge, this is the first report that details the apoptosis mechanism of 5-Aza-CdR treatment in the NCI–H1975 lung cancer cell line. Immunotherapies, particularly immune checkpoint inhibitors (ICIs), that targets programmed cell death 1 protein (PD-1)/programmed death-ligand1 (PD-L1) signaling pathway, have prompted a paradigm shift in cancer treatment, demonstrating significant efficacy and long-term clinical benefits in NSCLC (Carbone et al., 2017; Onoi et al., 2020). Despite the fact that ICIs have shown better overall survival in NSCLC, the response rate is approximately 20–30% (Onoi et al., 2020). Therefore, the need for other combined therapies to increase the response rate of patients is critical. We propose the use of 5-Aza-CdR as a potential pharmacological agent for future clinical trials in combination with ICIs to treat NSCLC patients owing to its ability to induce the expression of NY-ESO-1 antigen and to facilitate intrinsic and extrinsic apoptotic pathway mediated tumour cell killing and inhibition of tumour invasion.

The present study has a limitation as it was based only on *in vitro* cell lines demonstration which might fail to capture the inherent complexity of *in vivo* organ systems and not predict the *in vivo* responses. However, the data presented here shed the light on the important epigenetic and immunoregulatory effect of 5-Aza-CdR and this should pave the way for further *in vivo* studies that should aim to confirm and strengthen the

findings of our study.

5. Conclusion

We have used a novel proteomic approach to study the demethylating effect and mechanisms of 5-Aza-CdR treatment in a lung cancer cell line known for its sensitivity to upregulate the NY-ESO1 antigen. We confirmed that treatment with 5-Aza-CdR induces the expression of the NY-ESO-1 antigen, and we established the functionality of the apoptotic signaling system within the tumour cells to sensitize these cells to cell death via activation of intrinsic and extrinsic apoptotic pathways.

Credit author statement

Said Dermime: Conception, design, Formal analysis, interpretation, Manuscript writing, Final approval of manuscript, Varghese P Inchakalody: Conception, design, Collection and assembly of data, Formal analysis, interpretation, Manuscript writing, Final approval of manuscript, Roopesh Krishnankutty: Conception, design, Collection and assembly of data, Formal analysis, interpretation, Manuscript writing, Final approval of manuscript, Maysaloun Merhi: Conception, design, Formal analysis, interpretation, Manuscript writing, Final approval of manuscript, Varun Sasidharan Nair: Conception, design, Collection and assembly of data, Formal analysis, interpretation, Manuscript writing, Final approval of manuscript, Shahab Uddin: Conception, design, Formal analysis, interpretation, Manuscript writing, Final approval of manuscript, Eyad Elkord: Conception, design, Formal analysis, interpretation, Manuscript writing, Final approval of manuscript, Shereena P Hydrose: Collection and assembly of data, Formal analysis, interpretation, Manuscript writing, Final approval of manuscript, Lubna Therachiyil: Collection and assembly of data, Formal analysis, interpretation, Manuscript writing, Final approval of manuscript, Asma A Elashi: Collection and assembly of data, Formal analysis, interpretation, Manuscript writing, Final approval of manuscript, Abdul Q Khan: Collection and assembly of data, Manuscript writing, Final approval of manuscript, Sara Taleb: Collection and assembly of data, Formal analysis, interpretation, Manuscript writing, Final approval of manuscript, Afsheen Raza: Manuscript writing, Final approval of manuscript, Zeenath Safira K.M Yoosuf: Manuscript writing, Final approval of manuscript, Queenie Fernandes: Manuscript writing, Final approval of manuscript, Lobna Al-Zaidan: Manuscript writing, Final approval of manuscript, Sarra Mestiri: Manuscript writing, Final approval of manuscript, Nassiba Taib: Manuscript writing, Final approval of manuscript, Takwa Bedhiafi: Manuscript writing, Final approval of manuscript. Dina Moustafa: Manuscript writing, Final approval of manuscript, Laila Assami: Manuscript writing, Final approval of manuscript, Karama Makni Maalej: Manuscript writing, Final approval of manuscript, Ussama Al Homsi: Manuscript writing, Final approval of manuscript.

Funding

The Medical Research Center at Hamad Medical Corporation, Qatar supported this work under the approved project MRC-01-20-951.

Declaration of competing interest

The authors declare that they have no known competing financial interests or personal relationships that could have appeared to influence the work reported in this paper.

Data availability

Data will be made available on request.

Acknowledgment

Open access funding provided by Qatar National Library.

Appendix A. Supplementary data

Supplementary data to this article can be found online at https://doi.org/10.1016/j.ejphar.2023.175612.

References

Al-Alwan, M., Olabi, S., Ghebeh, H., Barhoush, E., Tulbah, A., Al-Tweigeri, T., Ajarim, D., Adra, C., 2011. Fascin is a key regulator of breast cancer invasion that acts via the modification of metastasis-associated molecules. PLoS One 6 e27339-e27339.

Almstedt, M., Blagitko-Dorfs, N., Duque-Afonso, J., Karbach, J., Pfeifer, D., Jäger, E., Lübbert, M., 2010. The DNA demethylating agent 5-aza-2'-deoxycytidine induces expression of NY-ESO-1 and other cancer/testis antigens in myeloid leukemia cells. Leuk. Res. 34, 899–905.

Aung, P.P., Liu, Y.-C., Ballester, L.Y., Robbins, P.F., Rosenberg, S.A., Lee, C.-C.R., 2014. Expression of New York esophageal squamous cell carcinoma-1 in primary and metastatic melanoma. Hum. Pathol. 45, 259–267.

Azad, N., Zahnow, C.A., Rudin, C.M., Baylin, S.B., 2013. The future of epigenetic therapy in solid tumours - lessons from the past. Nat. Rev. Clin. Oncol. 10, 256–266.

Bai, H., Wang, C., Qi, Y., Xu, J., Li, N., Chen, L., Jiang, B., Zhu, X., Zhang, H., Li, X., Yang, Q., Ma, J., Xu, Y., Ben, J., Chen, Q., 2019. Major vault protein suppresses lung cancer cell proliferation by inhibiting STAT3 signaling pathway. BMC Cancer 19, 454-454.

Bao, L., Dunham, K., Lucas, K., 2011. MAGE-A1, MAGE-A3, and NY-ESO-1 can be upregulated on neuroblastoma cells to facilitate cytotoxic T lymphocyte-mediated tumor cell killing. Cancer Immunol. Immunother. 60, 1299–1307.

Barrow, C., Browning, J., MacGregor, D., Davis, I.D., Sturrock, S., Jungbluth, A.A., Cebon, J., 2006. Tumor antigen expression in melanoma varies according to antigen and stage. Clin. Cancer Res. 12, 764–771.

Berr, A.L., Wiese, K., Santos, G.d., Davis, J.M., Koch, C.M., Anekalla, K.R., Kidd, M., Cheng, Y., Hu, Y.-S., Ridge, K.M., Department. Vimentin is required for tumor progression and metastasis in a mouse model of non-small cell lung cancer. https://doi.org/10.1101/2020.06.04.130963.

Carbajo-García, M.C., Corachán, A., Segura-Benitez, M., Monleón, J., Escrig, J., Faus, A., Pellicer, A., Cervelló, I., Ferrero, H., 2021. 5-aza-2′-deoxycitidine inhibits cell proliferation, extracellular matrix formation and Wnt/β-catenin pathway in human uterine leiomyomas. Reprod. Biol. Endocrinol. 19, 106-106.

Carbone, D.P., Reck, M., Paz-Ares, L., Creelan, B., Horn, L., Steins, M., Felip, E., van den Heuvel, M.M., Ciuleanu, T.E., Badin, F., Ready, N., Hiltermann, T.J.N., Nair, S., Juergens, R., Peters, S., Minenza, E., Wrangle, J.M., Rodriguez-Abreu, D., Borghaei, H., Blumenschein Jr., G.R., Villaruz, L.C., Havel, L., Krejci, J., Corral Jaime, J., Chang, H., Geese, W.J., Bhagavatheeswaran, P., Chen, A.C., Socinski, M. A., CheckMate, I., 2017. First-line nivolumab in stage IV or recurrent non-small-cell lung cancer. N. Engl. J. Med. 376, 2415–2426.

Cartron, P.-F., Blanquart, C., Hervouet, E., Gregoire, M., Vallette, F.M., 2013. HDAC1-mSin3a-NCOR1, Dnmt3b-HDAC1-Egr1 and Dnmt1-PCNA-UHRF1-G9a regulate the NY-ESO1 gene expression Pierre-Francois. Molecular Oncology 7.

Chen, J., Wu, L., Xu, H., Cheng, S., 2019. 5-Aza-CdR regulates RASSF1A by inhibiting DNMT1 to affect colon cancer cell proliferation, migration and apoptosis. Cancer Manag. Res. 11, 9517–9528.

Chen, Y.T., Scanlan, M.J., Sahin, U., Türeci, Ö., Gure, A.O., Tsang, S., Williamson, B., Stockert, E., Pfreundschuh, M., Old, L.J., 1997. A testicular antigen aberrantly expressed in human cancers detected by autologous antibody screening. Proc. Natl. Acad. Sci. U.S.A. 94, 1914–1918.

Chüeh, A.C., Liew, M.-S., Russell, P.A., Walkiewicz, M., Jayachandran, A., Starmans, M. H.W., Boutros, P.C., Wright, G., Barnett, S.A., Mariadason, J.M., John, T., 2017. Promoter hypomethylation of NY-ESO-1, association with clinicopathological features and PD-L1 expression in non-small cell lung cancer. Oncotarget 8, 74036–74048.

Cox, J., Neuhauser, N., Michalski, A., Scheltema, R.A., Olsen, J.V., Mann, M., 2011. Andromeda: a peptide search engine integrated into the MaxQuant environment. J. Proteome Res. 10, 1794–1805.

Dan, H., Zhang, S., Zhou, Y., Guan, Q., 2019. DNA methyltransferase inhibitors: catalysts for antitumour immune responses. OncoTargets Ther. 12, 10903–10916.

Elmore, S., 2007. Apoptosis: a review of programmed cell death. Toxicol. Pathol. 35, 495–516.

Gupta, A., Nuber, N., Esslinger, C., Wittenbrink, M., Treder, M., Landshammer, A., Noguchi, T., Kelly, M., Gnjatic, S., Ritter, E., von Boehmer, L., Nishikawa, H., Shiku, H., Old, L., Ritter, G., Knuth, A., van den Broek, M., 2013. A novel human-derived antibody against NY-ESO-1 improves the efficacy of chemotherapy. Cancer Immun. 13, 3.

Hassler, M.R., Klisaroska, A., Kollmann, K., Steiner, I., Bilban, M., Schiefer, A.-I., Sexl, V., Egger, G., 2012. Antineoplastic activity of the DNA methyltransferase inhibitor 5-aza-2′-deoxycytidine in anaplastic large cell lymphoma. Biochimie 94, 2297–2307.

Jiang, H., Wu, L., Mishra, M., Chawsheen, H.A., Wei, Q., 2014. Expression of peroxiredoxin 1 and 4 promotes human lung cancer malignancy. American journal of cancer research 4, 445–460.

Juergens, R.A., Wrangle, J., Vendetti, F.P., Murphy, S.C., Zhao, M., Coleman, B., Sebree, R., Rodgers, K., Hooker, C.M., Franco, N., Lee, B., Tsai, S., Delgado, I.E.,

Rudek, M.A., Belinsky, S.A., Herman, J.G., Baylin, S.B., Brock, M.V., Rudin, C.M., 2011. Combination epigenetic therapy has efficacy in patients with refractory advanced non-small cell lung cancer. Cancer Discov. 1, 598–607.
Kanwal, R., Gupta, S., 2012. Epigenetic modifications in cancer. Clin. Genet. 81, 303–311.
Kleczko, E.K., Kwak, J.W., Schenk, E.L., Nemenoff, R.A., 2019. Targeting the complement pathway as a therapeutic strategy in lung cancer. Front. Immunol. 10.
Klose, T., Abiatari, I., Samkharadze, T., De Oliveira, T., Jäger, C., Kiladze, M., Valkovskaya, N., Friess, H., Michalski, C.W., Kleeff, J., 2012. The actin binding protein destrin is associated with growth and perineural invasion of pancreatic cancer. Pancreatology 12, 350–357.
Li, L.C., Dahiya, R., 2002. MethPrimer: designing primers for methylation PCRs. Bioinformatics 18, 1427–1431.
Lin, K., He, S., He, L., Chen, J., Cheng, X., Zhang, G., Zhu, B., 2014. Complement component 3 is a prognostic factor of non-small cell lung cancer. Mol. Med. Rep. 10, 811–817.
Liu, H., Zhang, Y., Li, L., Cao, J., Guo, Y., Wu, Y., Gao, W., 2021. Fascin actin-bundling protein 1 in human cancer: promising biomarker or therapeutic target? Molecular Therapy - Oncolytics 20, 240–264.
Liu, J., Zhang, Y., Xie, Y.-S., Wang, F.-L., Zhang, L.-J., Deng, T., Luo, H.-S., 2012. 5-Aza-2'-deoxycytidine induces cytotoxicity in BGC-823 cells via DNA methyltransferase 1 and 3a independent of p53 status. Oncol. Rep. 28, 545–552.
Lu, Y., Chan, Y.T., Tan, H.Y., Li, S., Wang, N., Feng, Y., 2020. Epigenetic regulation in human cancer: the potential role of epi-drug in cancer therapy. Mol. Cancer 19, 1–16.
Lucken-Ardjomande, S., Martinou, J.C., 2005. Regulation of Bcl-2 proteins and of the permeability of the outer mitochondrial membrane. Comptes Rendus Biol. 328, 616–631.
Mahmood, N., Rabbani, S.A., 2019. DNA methylation readers and cancer: mechanistic and therapeutic applications. Front. Oncol. 9.
Meng, X., Sun, X., Liu, Z., He, Y., 2021. A novel era of cancer/testis antigen in cancer immunotherapy. Int. Immunopharm. 98, 107889-107889.
Merhi, M., Raza, A., Inchakalody, V.P., Nashwan, A.J.J., Allahverdi, N., Krishnankutty, R., Uddin, S., Zar Gul, A.R., Al Homsi, M.U., Dermime, S., 2018. Squamous cell carcinomas of the head and neck cancer response to programmed cell death protein-1 targeting and differential expression of immunological markers: a case report. Front. Immunol. 9, 1769.
Merhi, M., Raza, A., Inchakalody, V.P., Siveen, K.S., Kumar, D., Sahir, F., Mestiri, S., Hydrose, S., Allahverdi, N., Jalis, M., Relecom, A., Al Zaidan, L., Hamid, M.S.E., Mostafa, M., Gul, A.R.Z., Uddin, S., Al Homsi, M., Dermime, S., 2020. Persistent anti-NY-ESO-1-specific T cells and expression of differential biomarkers in a patient with metastatic gastric cancer benefiting from combined radioimmunotherapy treatment: a case report. J Immunother Cancer 8.
Natsume, A., Wakabayashi, T., Tsujimura, K., Shimato, S., Ito, M., Kuzushima, K., Kondo, Y., Sekido, Y., Kawatsura, H., Narita, Y., Yoshida, J., 2008. The DNA demethylating agent 5-aza-2′-deoxycytidine activates NY-ESO-1 antigenicity in orthotopic human glioma. Int. J. Cancer 122, 2542–2553.
Nervi, C., De Marinis, E., Codacci-Pisanelli, G., 2015. Epigenetic treatment of solid tumours: a review of clinical trials. Clin. Epigenet. 7, 127.
Nicolussi, A., D'Inzeo, S., Capalbo, C., Giannini, G., Coppa, A., 2017. The role of peroxiredoxins in cancer. Molecular and Clinical Oncology 6, 139–153.
Onoi, K., Chihara, Y., Uchino, J., Shimamoto, T., Morimoto, Y., Iwasaku, M., Kaneko, Y., Yamada, T., Takayama, K., 2020. Immune checkpoint inhibitors for lung cancer treatment: a review. J. Clin. Med. 9.
Pathan, M., Keerthikumar, S., Ang, C.S., Gangoda, L., Quek, C.Y.J., Williamson, N.A., Mouradov, D., Sieber, O.M., Simpson, R.J., Salim, A., Bacic, A., Hill, A.F., Stroud, D. A., Ryan, M.T., Agbinya, J.I., Mariadason, J.M., Burgess, A.W., Mathivanan, S., 2015. FunRich: an open access standalone functional enrichment and interaction network analysis tool. Proteomics 15, 2597–2601.
Rappsilber, J., Mann, M., Ishihama, Y., 2007. Protocol for micro-purification, enrichment, pre-fractionation and storage of peptides for proteomics using StageTips. Nat. Protoc. 2, 1896–1906.
Raza, A., Merhi, M., Inchakalody, V.P., Krishnankutty, R., Relecom, A., Uddin, S., Dermime, S., 2020. Unleashing the immune response to NY-ESO-1 cancer testis antigen as a potential target for cancer immunotherapy. J. Transl. Med. 18, 140.
Revel, M., Daugan, M., Sautés-Fridman, C., Fridman, W., Roumenina, L., 2020. Complement system: promoter or suppressor of cancer progression? Antibodies 9, 57-57.
Sasidharan Nair, V., El Salhat, H., Taha, R.Z., John, A., Ali, B.R., Elkord, E., 2018. DNA methylation and repressive H3K9 and H3K27 trimethylation in the promoter regions of PD-1, CTLA-4, TIM-3, LAG-3, TIGIT, and PD-L1 genes in human primary breast cancer. Clin. Epigenet. 10, 1–12.
Satelli, A., Li, S., 2011. Vimentin in cancer and its potential as a molecular target for cancer therapy. Cell. Mol. Life Sci. : CM 68, 3033–3046.
Shoshan-Barmatz, V., De, S., Meir, A., 2017. The mitochondrial voltage-dependent anion channel 1, Ca2+ transport, apoptosis, and their regulation. Front. Oncol. 7, 1–12.
Sugita, Y., Wada, H., Fujita, S., Nakata, T., Sato, S., Noguchi, Y., Jungbluth, A.A., Yamaguchi, M., Chen, Y.-T., Stockert, E., Gnjatic, S., Williamson, B., Scanlan, M.J., Ono, T., Sakita, I., Yasui, M., Miyoshi, Y., Tamaki, Y., Matsuura, N., Noguchi, S., Old, L.J., Nakayama, E., Monden, M., 2004. NY-ESO-1 expression and immunogenicity in malignant and benign breast tumors. Cancer Res. 64, 2199. LP-2204.
Sung, H., Ferlay, J., Siegel, R.L., Laversanne, M., Soerjomataram, I., Jemal, A., Bray, F., 2021. Global cancer statistics 2020: GLOBOCAN estimates of incidence and mortality worldwide for 36 cancers in 185 countries. CA A Cancer J. Clin. 71, 209–249.
Thai, A.A., Solomon, B.J., Sequist, L.V., Gainor, J.F., Heist, R.S., 2021. Lung cancer. Lancet 398, 535–554.
Thomas, R., Al-Khadairi, G., Roelands, J., Hendrickx, W., Dermime, S., Bedognetti, D., Decock, J., 2018. NY-ESO-1 based immunotherapy of cancer: current perspectives. Front. Immunol. 9, 947.
Tyanova, S., Temu, T., Cox, J., 2016. The MaxQuant computational platform for mass spectrometry-based shotgun proteomics. Nat. Protoc. 11, 2301–2319.
Van Rechem, C., Black, J.C., Boukhali, M., Aryee, M.J., Graslund, S., Haas, W., Benes, C. H., Whetstine, J.R., 2015. Lysine demethylase KDM4A associates with translation machinery and regulates protein synthesis. Cancer Discov. 5, 255–263.
Velazquez, E.F., Jungbluth, A.A., Yancovitz, M., Gnjatic, S., Adams, S., O'Neill, D., Zavilevich, K., Albukh, T., Christos, P., Mazumdar, M., Pavlick, A., Polsky, D., Shapiro, R., Berman, R., Spira, J., Busam, K., Osman, I., Bhardwaj, N., 2007. Expression of the cancer/testis antigen NY-ESO-1 in primary and metastatic malignant melanoma (MM)–correlation with prognostic factors. Cancer Immun. 7, 11-11.
Viktorsson, K., Lewensohn, R., 2007. Apoptotic signaling pathways in lung cancer. J. Thorac. Oncol. 2, 175–179.
Wang, C., Youle, R.J., 2009. The role of mitochondria in apoptosis. Annu. Rev. Genet. 43, 95–118.
Weerasinghe, P., Garcia, G.E., Zhu, Q., Yuan, P., Feng, L., Mao, L., Jing, N., 2007. Inhibition of Stat3 activation and tumor growth suppression of non-small cell lung cancer by G-quartet oligonucleotides. Int. J. Oncol. 31, 129–136.
Wu, J., Liu, T., Rios, Z., Mei, Q., Lin, X., Cao, S., 2017. Heat shock proteins and cancer. Trends Pharmacol. Sci. 38, 226–256.
Zhang, Y.-G., Niu, J.-T., Wu, H.-W., Si, X.-L., Zhang, S.-J., Li, D.-H., Bian, T.-T., Li, Y.-F., Yan, X.-K., 2021. Actin-binding proteins as potential biomarkers for chronic inflammation-induced cancer diagnosis and therapy. Anal. Cell Pathol. 2021, 6692811-6692811.